

Metrological characterization of instruments for body impedance analysis

Valerio Marcotuli¹, Matteo Zago², Alex P. Moorhead¹, Marco Vespasiani³, Giacomo Vespasiani³, Marco Tarabini¹

¹ Department of Mechanical Engineering, Politecnico di Milano, via Privata Giuseppe La Masa 1, 20156 Milan, Italy

² Faculty of Exercise and Sports Science, Università degli Studi di Milano, Via Festa del Perdono 7 - 20122 Milan, Italy

³ Technical Department, Metadieta s.r.l., Via Antonio Bosio, 2, 00161 Rome, Italy

ABSTRACT

Body impedance analysis (BIA) is used to evaluate the human body composition by measuring the resistance and reactance of human tissues with a high-frequency, low-intensity electric current. Nonetheless, the estimation of the body composition is influenced by many factors: body status, environmental conditions, instrumentation, and measurement procedure. This work studies the effect of the connection cables, conductive electrodes, adhesive gel, and BIA device characteristics on the measurement uncertainty. Tests were initially performed on electric circuits with passive elements and on a jelly phantom simulating the body characteristics. Results showed that the cables mainly contribute to increase the error on the resistance measurement, while the electrodes and the adhesive introduce a negligible disturbance on the measurement chain. This paper also proposes a calibration procedure based on a multivariate linear regression to compensate for the systematic error effect of BIA devices.

Section: RESEARCH PAPER

Keywords: Bioimpedance; body composition; measurement uncertainty; calibration; multivariate linear regression

Citation: Valerio Marcotuli, Matteo Zago, Alex P. Moorhead, Marco Vespasiani, Giacomo Vespasiani, Marco Tarabini, Metrological characterization of instruments for body impedance analysis, Acta IMEKO, vol. 11, no. 3, article 14, September 2022, identifier: IMEKO-ACTA-11 (2022)-03-14

Section Editor: Francesco Lamonaca, University of Calabria, Italy

Received October 7, 2021; **In final form** August 31, 2022; **Published** September 2022

Copyright: This is an open-access article distributed under the terms of the Creative Commons Attribution 3.0 License, which permits unrestricted use, distribution, and reproduction in any medium, provided the original author and source are credited.

Corresponding author: Valerio Marcotuli, e-mail: valerio.marcotuli@polimi.it

1. INTRODUCTION

Body composition describes the main components of the human body in terms of free fat mass (FFM), fat mass (FM) or their ratio FFM/FM. The analysis of body composition is used in different fields such as biology and medicine to estimate the nutritional status, muscular volume variations and potentially event pathological status. For example, physiological aging leads to a reduction of FFM and muscular mass, while fat increases and is redistributed over the body areas [1].

Different levels of body composition, atomic, molecular cellular, tissular and global, can be analyzed depending on the measurement methods [2]. Body mass index (BMI) is a generic indicator of the body composition, but it tends to give inaccurate information when subjects are highly overweight or obese; in fact, it is possible that malnutrition exists yet is masked by the high amount of fat mass [3].

A solution for measuring body composition is represented by the Dual-energy X-ray Absorptiometry (DXA). This is an imaging technique, similar to Magnetic Resonance Imaging (MRI), which scans the patient with two beams of x-rays with different energy (usually 40 and 70 kV). In recent years, DXA has become recognized as the “gold standard” for measuring body composition [4]. It evaluates both the global and the regional distribution of the three main body components: bone mineral content (BMC), FM and FFM. The accuracy of DXA makes it very effective in studying patient composition within specific body regions and evaluating their effect on the patient health [5]. Unfortunately, a DXA machine is expensive (\$20,000+) making it typically available only at big infrastructure such as clinics and hospitals. An alternative technique is the Bioelectrical Impedance Analysis (BIA): this employs a low alternate current (AC) with high frequency at 50 kHz transmitted across the body to estimate its composition based on the hydration level of tissues [6]. BIA allows for quick examinations, and it is much less expensive than DXA. Additionally, BIA is less dangerous than DXA as it does

not use x-rays, meaning it can be also repeated several times with no contraindications. Nevertheless, BIA can be highly affected by many factors such as altered hydration of the subject, measurement conditions, ethnic background, and health conditions [7].

BIA devices measure the magnitude of the impedance opposed to the current that varies with respect to the body anatomy. Specifically, the physical principle assumes that the body is made up of tissues with different composition. Some tissues are good conductors due to their water content while others are insulators. The water content is inversely related to the resistance that opposes the current flow. On the other hand, cellular membranes, able to accumulate electrical loads, can be considered capacitors. The presence of capacitors is directly proportional to reactance and introduces an observable delay on the current flow. The sum of the resistance and reactance defines the impedance. Its evaluation indicates the body hydration and provides an estimate of the nutritional state equivalent to the cellular amount. Since water is the main component of the cells and it is almost absent in fat, it is possible to deduce the amount of FFM from the water content. Consequently, FM is evaluated by simply subtracting the FFM to the total weight [8].

1.1. Fricke's Circuit: a human body electrical model

The human body can be modeled as a set of resistance and capacitance connected in parallel or in series. The most common body model used in the field of BIA is the *Fricke's circuit*, whose two parallel branches represent the intracellular and extracellular components. In this model, a high-frequency current passes through the intracellular water, while at low frequencies through the extracellular space. This is because at zero or low frequency, the current does not penetrate the cell membrane (acting as an insulator), while it passes through the extracellular medium made of water and sodium [9].

The intracellular behavior, in turn, can be modeled as a resistance R_i (due to the water and potassium content) and a capacitance X_c of the cell membrane, while the extracellular behavior is described by a single resistance R_e as shown in Figure 1. The total body resistance R measured by a BIA instrument is in turn a combination of the two resistances R_i and R_e which indicate the real part of a complex number [10]. Generally, the phasor and other indices such the ratio R_i/R_e can be good estimators of diseases presence, nutritional status, and hydration condition [11].

1.2. The calibration plots

The Cole-Cole plot is commonly used to visualize the electrical response of body measurements with the resistance R on the x-axis and the negative reactance X_c on the y-axis. At

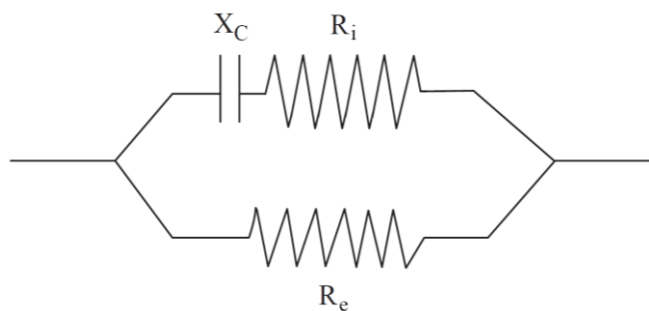


Figure 1. Fricke's circuit model for body composition consisting into two branches related to the intracellular and extracellular behaviors.

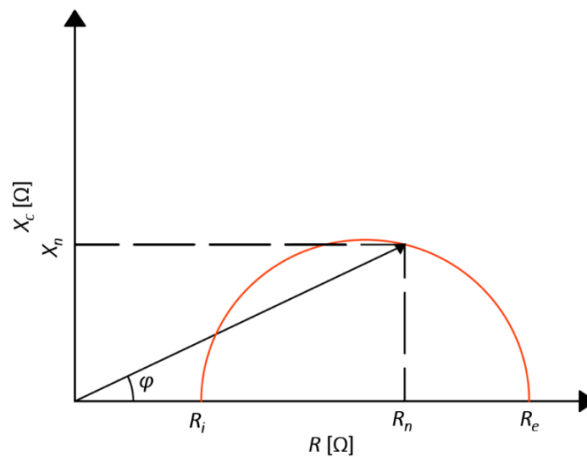


Figure 2. Example of Cole-Cole plot of the Fricke's circuit.

extremely high or ideally infinite frequency, the intracellular branch is the only one with the minimum resistance value R_i .

At low or zero frequency, the current passes only in the extracellular space since the cell membranes act as insulators. Consequently, R_e is the maximum value of resistance. The relationship between the capacitance X_c and the total resistance R of a body can be expressed by a phase angle φ [12]. Therefore, the resulting phasor ranging from R_i and R_e describes an arc segment as shown in Figure 2 and all the measured values would lie below it. This plot can be standardized with respect to height, gender, and ethnicity, to form a calibration model divided into adjacent areas contained in tolerance ellipses at 50 %, 75 %, and 95 % belonging to a certain population group (as seen in Figure 3, which shows an example of a calibration model standardized by the height, h) [13].

The plot is used as a calibration map by companies for converting a measurement performed by means of a device into a body status information [14]. If the BIA device displays a low measurement accuracy, measurement results could be misleading.

1.3. Measurement uncertainty

The biasing factors on bioimpedance estimation can be attributed to the subject (the measurand is not constant), to the measurement protocols, and to the instrumentation [15]. In this

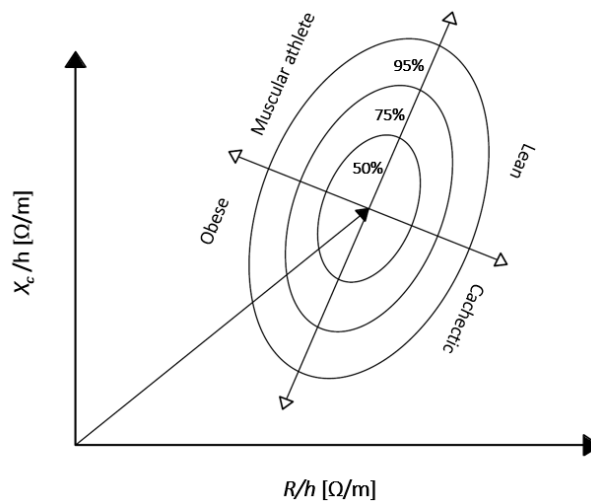


Figure 3. Example of a calibration model standardized by the height (h).

study we investigate the possible source of errors of the BIA instrumentation, consisting in a control unit, cables, and electrodes.

The control unit is composed of electronic circuitry placed in a case with one or more ports for connecting the cables. Even if protected, the circuitry is subjected to thermal, electrical, and magnetic disturbances [16], [17]. The identification of these disturbances is essential for the performances of the devices and to improve competitiveness in the market. For this reason, the control unit and the accessories should be metrologically characterized through a specific test for each possible source of error [18], [19]. Moreover, if the disturbances are properly identified, a corrective calibration strategy can be applied [20], [21].

2. MATERIALS AND METHODS

2.1. Instrumental equipment

The instrumentation selected for this study consists of a BIA device (*Metadieta Bia*), three sets of cables, three sets of electrodes of different manufacturers, a series of resistances and capacitors, and a breadboard.

Metadieta Bia (Figure 4) is an electromedical device for the evaluation of the corporal composition manufactured by the company Meteda S.r.l. (Rome, Italy). The bioimpedance is measured by placing four electrodes on the hands and feet, with a single cable connected to the main unit. The impedance value is computed from the response to a sinusoidal current of 350 μ A with a frequency of 50 kHz (a *standard de facto* for most BIA devices with a single frequency). The device has a size of 43 \times 43 \times 12 mm³ and a mass of 50 g; a lithium battery can supply the device up to 14 hours in working conditions. It does not have a screen on the control unit, but it can be managed by an application running on phones, tablets, and computers with a Bluetooth connection. The device is designed to be used in clinics by physicians, nutritional biologists and qualified sanitary personnel but also by consumers in home environment.

The application provides the user with information about the preparation and the execution of the test measurement, then it sends and stores the data on the cloud for later analyses. Data measurements are processed on the cloud application and the results can be either quantitative for clinical personnel or qualitative with displayed information in graphs along with the tendencies for individual users.

The additional equipment for the test is represented by three cables of the same model between the main unit and the four



Figure 4. Picture of the Metadieta Bia control unit.

electrodes clamps and a series of electrodes of three producers: Biatrodes® by Akern slr (Firenze, Italy), BIA Electrodes by RJL Systems Inc (Clinton Twp, MI, USA), and Regal™ resting ECG by Vermed® Inc (Bells Falls, VT, USA).

2.2. Proposed method

The first operation to perform with a measurement device regards the metrological characterization in terms of repeatability and reproducibility after the identification of the possible sources of error [22]. Generally, this kind of device makes use of empirical equations whose parameters are established by means of a calibration operation performed in laboratory [23]. Since the calibration curves can assume a large set of values, a simplification of the process can rely on the study of a group of key values.

This research proposes a data selection based on six values of resistance between 200 Ω and 900 Ω with a step of 140 Ω , combined with six values of reactance between 15 Ω and 115 Ω with a step of 20 Ω . These values are represented in the grid in Figure 5.

To assemble a physical circuit starting from the reactance values, suitable capacitors can be identified by converting X_c into a capacitance C with the formula:

$$C = \frac{1}{2 \cdot \pi \cdot f \cdot X_c}, \quad (1)$$

where f is the frequency of AC generated by the Metadieta Bia device, i.e. 50 kHz. The capacitance values obtained after the conversion are therefore: 212 nF, 91 nF, 58 nF, 42 nF, 34 nF, and 28 nF.

By combining the values of resistance and capacitance, we defined a grid of 36 combinations and we evaluated the measurements' repeatability and reproducibility in each condition. The procedure also allows identifying compensation functions allowing to reduce the systematic errors affecting the reading [24].

2.3. Experimental design

The Metadieta Bia is turned on when the cables are inserted in the miniUSB port and the connection is initiated by the application on a master device.

Measurements are typically performed by placing four electrodes on the hands and feet. The electrodes are silver plated for a low resistance and attached to the skin using an adhesive gel. However, for consistency, all the experiments were performed on laboratory instrumentation with electric circuits

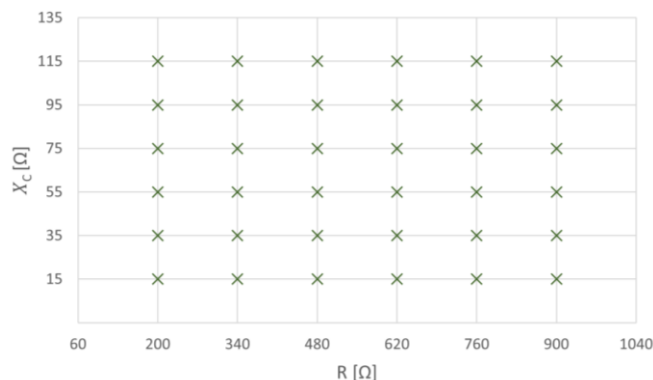


Figure 5. Calibration grid with 36 combinations of the key values selected.

Table 1. Resistances and capacitances of the selected components and the reactance values after conversion for the calibration map experiments.

Component	1	2	3	4	5	6
R in Ω	200	330	470	615	780	910
C in nF	225	92	51	36	32	27
X_c in Ω	14	35	56	89	99	120

representing the body composition through the Fricke’s model, so the electrodes were included only in specific tests.

The tests were performed in MetroSpace Lab of Politecnico di Milano and can be divided into:

1. Preliminary tests for the metrological characterization of Metadieta Bia device, cables, electrodes, and adhesive gel.
2. Test for systematic error compensation based on the calibration grid in Figure 5.

A high precision LCR meter, model LCR-819 GW Instek (Good Will Instrument Co., Ltd, Taiwan), was used as a reference system for measuring the impedance of the test components, while a multimeter, model Agilent 34401A, was used for the only resistance measurements of the electrical components.

2.4. Preliminary tests

First, the measurement repeatability of the control unit was tested by performing 30 measurements of the resistance R and reactance X_c repeated on five different electric circuits connecting the cable clamps directly to the circuit with no other modifications between each test and the next.

The three different cables of the same model were tested with 30 measurements each with the LCR meter, on the same electric circuit directly connecting the clamps of the cables.

Keeping the same configuration, the effect of the electrodes was studied applying these components without the adhesive material between the clamps and the electric circuit with passive elements.

A total of 30 different sets of electrodes of the three manufacturers were tested, 4 electrodes for each set. At the same time, the resistance R of the cables and the electrodes was measured 30 times for each component through the multimeter. The variability of electrical resistance of the electrodes was estimated by placing the multimeter terminals in two positions, on the tab and on an opposite area far from it (circled in Figure 6).

The effect of the adhesive gel, which determines the interaction with the BIA device and a biological tissue, was simulated by means of a jelly phantom (Figure 7) with nominal



Figure 6. Area of the electrode for measuring the resistance.

resistance of $R^{ph} = (571.2 \pm 1.2) \Omega$ (C.I. = 68 %) and nominal reactance of $X_c^{ph} = (75.1 \pm 1.9) \Omega$ (C.I. = 68 %) [25].

For this test, 30 measurements for each manufacturer’s electrode were performed to calculate the mean value of the resistance \bar{R} and reactance \bar{X}_c and the relative standard deviation. The four electrodes were positioned at the edges of the container, one couple on the left side and the other couple on the right side with a distance of about 30 cm. The distance between the two electrodes of each couple was of about 10 cm as recommended by the manufacturer.

This configuration with the dominant distance (30 cm > 10 cm) between the two couples of electrodes aimed to replicate the measurement behaviour on a human body, avoiding uncontrolled dispersion of the electric charge.

2.5. Tests for systematic error compensation

A set of 36 circuits with passive elements was built by combining selected components with the resistance and capacitance collected in Table 1, to the key values of the calibration grid in Figure 5. Table 1 also includes the reactance values after the conversion obtained by inverting the Eq.1.

The resistances components have a manufacturing tolerance of 0.1%, whereas the capacitors have a value of 1%. The circuits were mounted on a breadboard and the values read by Metadieta Bia device were compared to the values read by the LCR meter as references [26].

The differences between the measured and the reference allowed to calculate the RMSE and control for the presence of defined patterns related to systematic disturbances. Part of these disturbances was removed by adding two corrections terms R^a and X_c^g , obtained by a least square minimization of a multivariate linear model, to the generic measurements R and X_c in the form:

$$R^{adj} = R + R_a \quad (2)$$

and

$$X_c^{adj} = X_c + X_c^a, \quad (3)$$

where R^{adj} and X_c^{adj} are the compensated results.



Figure 7. Preliminary test of the electrodes on a jelly phantom.

3. RESULTS

3.1. Preliminary tests

The results of the repeatability test of the control unit on the 5 electric circuits with 30 measurements performed on each circuit are shown in Table 2: R and X_c are the key values chosen for the experiments, R^{ref} and X_c^{ref} are the reference values read by the LCR meter, \bar{R} and \bar{X}_c are the mean values read by the Metadieta Bia device with σ_R and σ_{X_c} the relative standard deviations.

The three tested cables showed a standard deviation of the resistance of $\sigma_R = 1.8 \Omega$, while the standard deviation of the reactance is $\sigma_{X_c} = 0.1 \Omega$. From these values it was possible to evaluate the uncertainty values $u_R = \sigma_R/\sqrt{30} = 0.33 \Omega$ and $u_{X_c} = \sigma_{X_c}/\sqrt{30} = 0.018 \Omega$ (C.I. = 68 %).

The electrode without the adhesive gel were tested on a circuit with the nominal resistance $R = (617.812 \pm 0.011) \Omega$ (C.I. = 68 %) and the equivalent reactance $X_c = (90.137 \pm 0.019) \Omega$ (C.I. = 68 %) with the Metadieta Bia device. The mean and the standard deviation of the resistance and the reactance are reported in Table 3. The maximum standard deviation values were reported by the RJL systems electrodes equal to $\sigma_R = 0.5 \Omega$ and $\sigma_{X_c} = 0.1 \Omega$ with the correspondent uncertainties equal to $u_R = \sigma_R/\sqrt{30} = 0.091 \Omega$ and $u_{X_c} = \sigma_{X_c}/\sqrt{30} = 0.018 \Omega$ (C.I. = 68 %).

The resistance-only measurements of the same electrodes performed through the multimeter are reported in Table 4. In this case both RJL systems and Vermed® electrodes reported a

maximum standard deviation of $\sigma_R = 0.4 \Omega$ and an uncertainty of $u_R = \sigma_R/\sqrt{30} = 0.073 \Omega$ (C.I. = 68 %).

The last experiment of the preliminary test on the jelly phantom are reported in Table 5. All three electrode samples showed a standard deviation of $\sigma_R = 0.1 \Omega$ with an uncertainty of $u_R = \sigma_R/\sqrt{30} = 0.018 \Omega$ (C.I. = 68 %), whereas Akern and Vermed® electrodes reported a standard deviation different from zero and equal to $\sigma_{X_c} = 0.1 \Omega$ corresponding to an uncertainty of $u_{X_c} = \sigma_{X_c}/\sqrt{30} = 0.018 \Omega$ (C.I. = 68 %).

3.2. Systematic error compensation

The measurements on 36 electric combinations with the Metadieta Bia device and the reference values are depicted in Figure 8.

From these data, the RMSE of the 36 configurations resulted $R_{RMSE} = 4.17 \Omega$ and $X_{c,RMSE} = 7.28 \Omega$. The minimization of the least square on the multivariate linear regression returned the following correction terms:

$$R^a = -1.592 + 0.994 \cdot R + 0.002 \cdot X_c + 2.45 \cdot 10^{-5} \cdot R \cdot X_c \quad (4)$$

and

$$X_c^a = -3.412 + 0.010 \cdot R + 1.079 \cdot X_c - 2.19 \cdot 10^{-5} \cdot R \cdot X_c \quad (5)$$

with R and X_c the actual values read by the BIA device. Furthermore, the multivariate linear regression reported the

Table 2. Results of the repeatability test of the control unit on 5 electric circuits.

R in Ω	X_c in Ω	R^{ref} in Ω	X_c^{ref} in Ω	\bar{R} in Ω	σ_R in Ω	\bar{X}_c in Ω	σ_{X_c} in Ω
200	15	200.1	17.9	202.7	0.0	18.9	0.1
200	75	191.4	92.3	193.5	0.1	88.7	0.1
340	115	330.5	124.4	333.4	0.1	116.1	0.0
620	75	617.8	90.1	622.1	0.0	80.2	0.0
900	95	910.9	101.1	916.9	0.0	98.3	0.0

Table 3. Results of the repeatability test of the three producer's electrodes without the adhesive gel by the Metadieta Bia device.

Manufacturer	\bar{R} in Ω	σ_R in Ω	\bar{X}_c in Ω	σ_{X_c} in Ω
Akern	619.2	0.2	91.4	0.0
RJL Systems	619.5	0.5	91.4	0.1
Vermed®	619.4	0.1	91.5	0.0

Table 4. Results of the repeatability test of the three producer's electrodes without the adhesive gel by the multimeter Agilent 34401A.

Manufacturer	\bar{R} in Ω	σ_R in Ω
Akern	1.6	0.3
RJL Systems	2.1	0.4
Vermed®	2.1	0.4

Table 5. Results of the repeatability test of the three producer's electrodes with the adhesive gel on the jelly phantom by the Metadieta Bia device.

Manufacturer	\bar{R} in Ω	σ_R in Ω	\bar{X}_c in Ω	σ_{X_c} in Ω
Akern	573.2	0.1	79.1	0.1
RJL Systems	573.3	0.1	78.5	0.0
Vermed®	573.2	0.1	78.9	0.1

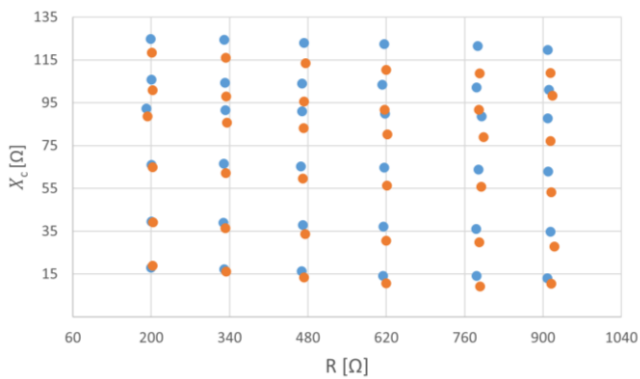


Figure 8. Comparison between the reference values provided by the LCR meter (blue dots) and the measurements performed with the Metadieta Bia device (orange dots).

adjusted R^2 values of $\bar{R}_R^2 = 0.947$ for the resistance and $\bar{R}_{Xc}^2 = 0.696$ for the reactance. Compensating for the values in Figure 8 with the terms R^a and X_c^a , the values of RMSE decrease to $R_{RMSE} = 1.16 \Omega$ and $X_{c,RMSE} = 1.28 \Omega$.

4. DISCUSSION

The tests on the Metadieta Bia device revealed that the cables, the silver-plated electrodes, and the gel have a negligible influence on the overall measurement chain: the cables showed an uncertainty of $u_R = 3.3 \cdot 10^{-1} \Omega$ (C.I. = 68 %) and $u_{Xc} = 1.8 \cdot 10^{-2} \Omega$ (C.I. = 68 %), while the maximum uncertainties introduced by the electrodes were $u_R = 8.6 \cdot 10^{-2} \Omega$ (C.I. = 68 %) and $u_{Xc} = 1.7 \cdot 10^{-2} \Omega$ (C.I. = 68 %). The comparison between the three electrode models also showed that these elements have the same electric characteristics for which the device performance does not change, as proved by Sanchez et Al. [27]. Also, the tests for the gel on the jelly phantom did not report any significant influence since the maximum uncertainties were $u_R = 1.7 \cdot 10^{-2} \Omega$ (C.I. = 68 %) and $u_{Xc} = 1.7 \cdot 10^{-2} \Omega$ (C.I. = 68 %). This means that the adhesive gel is essential for keeping the contact between the electrodes and the skin but it does not add any relevant disturbance to the measurement process [28].

The comparison between the reference values and the measurements with the BIA device in Figure 8 showed that the uncertainties of the reactance and resistance tend to increase for the combinations with higher values. Nonetheless, the trend was corrected effectively by the multivariate linear regression. In fact, the two terms R^a and X_c^a can decrease the uncertainties to $R_{RMSE} = 1.16 \Omega$ and $X_{c,RMSE} = 1.28 \Omega$. Moreover, by observing the expressions of R^a , it is evident that the read reactance contribution is negligible. Conversely, the read resistance value has a relevant influence on the compensation procedure.

5. CONCLUSIONS

BIA is an effective and valid tool to estimate body composition from a fast and safe single measurement. Nonetheless, the estimation can fail when the measurement conditions change or if there is a poor calibration of the BIA device. In this paper, we evaluated the causes of variability of bioimpedance measurements. First, the equipment was metrologically characterized showing that it does not influence the measurements significantly with uncertainties lower than 0.35Ω (C.I. = 68 %) for both resistance and reactance.

For what concerns the validation of BIA equations, it must be carried out against gold standards, even though they exhibit limitations due to hydration conditions, age, and ethnicity. This study proposed a calibration grid made of 36 configurations of key values. The grid allowed to calculate multivariate linear models minimizing the least square errors which can be used to calibrate the Metadieta Bia device.

In the case-study presented in this work, the bias error compensation reduced the RMSE from 4.2Ω to 1.2Ω for the resistance and from 7.3Ω to 1.3Ω for the reactance with the adjusted R^2 values respectively of 0.947 and 0.696. Prospectively, the calibration maps can be extended to higher values and the key points grid can be further populated for more robust results.

REFERENCES

- [1] U. G. Kyle, L. Genton, D. O. Slosman, C. Pichard, Fat-free and fat mass percentiles in 5225 healthy subjects aged 15 to 98 years, *Nutrition*. 17 (2001), pp. 534-541. DOI: [10.1016/S0899-9007\(01\)00555-X](https://doi.org/10.1016/S0899-9007(01)00555-X)
- [2] H. C. Lukaski, Methods for the assessment of human body composition: Traditional and new, *Am. J. Clin. Nutr.* 46 (1987), pp. 537-556. DOI: [10.1093/ajcn/46.4.537](https://doi.org/10.1093/ajcn/46.4.537)
- [3] A. Talluri, R. Liedtke, E. I. Mohamed, C. Maiolo, R. Martinoli, A. De Lorenzo, The application of body cell mass index for studying muscle mass changes in health and disease conditions, *Acta Diabetol.* 40 (2003). DOI: [10.1007/s00592-003-0088-9](https://doi.org/10.1007/s00592-003-0088-9)
- [4] A. Choi, J. Y. Kim, S. Jo, J. H. Jee, S. B. Heymsfield, Y. A. Bhagat, I. Kim, J. Cho, Smartphone-based bioelectrical impedance analysis devices for daily obesity management, *Sensors (Switzerland)*. 15 (2015), pp. 22151-22166. DOI: [10.3390/s150922151](https://doi.org/10.3390/s150922151)
- [5] P. Pisani, A. Greco, F. Conversano, M. D. Renna, E. Casciaro, L. Quarta, D. Costanza, M. Muratore, S. Casciaro, A quantitative ultrasound approach to estimate bone fragility: A first comparison with dual X-ray absorptiometry, *Meas. J. Int. Meas. Confed.* 101 (2017), pp. 243-249. DOI: [10.1016/j.measurement.2016.07.033](https://doi.org/10.1016/j.measurement.2016.07.033)
- [6] M. Dehghan, A. T. Merchant, Is bioelectrical impedance accurate for use in large epidemiological studies?, *Nutr. J.* 7 (2008), pp. 1-7. DOI: [10.1186/1475-2891-7-26](https://doi.org/10.1186/1475-2891-7-26)
- [7] U. G. Kyle, I. Bosaeus, A. D. De Lorenzo, P. Deurenberg, M. Elia, J. M. Gómez, B. L. Heitmann, L. Kent-Smith, J. C. Melchior, M. Pirlich, H. Scharfetter, A. M. W. J. Schols, C. Pichard, Bioelectrical impedance analysis - Part II: Utilization in clinical practice, *Clin. Nutr.* 23 (2004), pp. 1430-1453. DOI: [10.1016/j.clnu.2004.09.012](https://doi.org/10.1016/j.clnu.2004.09.012)
- [8] J. Hlubik, P. Hlubik, L. Lhotska, Bioimpedance in medicine: Measuring hydration influence, *J. Phys. Conf. Ser.* 224 (2010), 012135. DOI: [10.1088/1742-6596/224/1/012135](https://doi.org/10.1088/1742-6596/224/1/012135)
- [9] F. Villa, A. Magnani, M. A. Maggioni, A. Stahn, S. Rampichini, G. Merati, P. Castiglioni, Wearable multi-frequency and multi-segment bioelectrical impedance spectroscopy for unobtrusively tracking body fluid shifts during physical activity in real-field applications: A preliminary study, *Sensors (Switzerland)*. 16 (2016), pp. 1-15. DOI: [10.3390/s16050673](https://doi.org/10.3390/s16050673)
- [10] I. V. Krivtsov, I. V. Pentegov, V. N. Sydoretz, S. V. Rymar, A Technique for Experimental Data Processing At Modeling the Dispersion of the Biological Tissue Impedance Using the Fricke Equivalent Circuit, *Electr. Eng. Electromechanics*. 0 (2017), pp. 27-37. DOI: [10.20998/2074-272x.2017.5.04](https://doi.org/10.20998/2074-272x.2017.5.04)

- [11] S. Cigarrán Guldrís, Future uses of vectorial bioimpedance (BIVA) in nephrology, *Nefrologia*. 31 (2011), pp. 635-643.
DOI: [10.3265/Nefrologia.pre2011.Oct.11108](https://doi.org/10.3265/Nefrologia.pre2011.Oct.11108)
- [12] F. Savino, F. Cresi, G. Grasso, R. Oggero, L. Silvestro, The biagram vector: A graphical relation between reactance and phase angle measured by bioelectrical analysis in infants, *Ann. Nutr. Metab.* 48 (2004), pp. 84-89.
DOI: [10.1159/000077042](https://doi.org/10.1159/000077042)
- [13] R. González-Landaeta, O. Casas, R. Pallàs-Areny, Heart rate detection from plantar bioimpedance measurements, *IEEE Trans. Biomed. Eng.* 55 (2008), pp. 1163-1167.
DOI: [10.1109/TBME.2007.906516](https://doi.org/10.1109/TBME.2007.906516)
- [14] F. Ibrahim, M. N. Taib, W. A. B. Wan Abas, C. C. Guan, S. Sulaiman, A novel approach to classify risk in dengue hemorrhagic fever (DHF) using bioelectrical impedance analysis (BIA), *IEEE Trans. Instrum. Meas.* 54 (2005), pp. 237-244.
DOI: [10.1109/TIM.2004.840237](https://doi.org/10.1109/TIM.2004.840237)
- [15] S. F. Khalil, M. S. Mohktar, F. Ibrahim, The theory and fundamentals of bioimpedance analysis in clinical status monitoring and diagnosis of diseases, *Sensors (Switzerland)*. 14 (2014), pp. 10895-10928.
DOI: [10.3390/s140610895](https://doi.org/10.3390/s140610895)
- [16] A. Ferrero, Measuring electric power quality: Problems and perspectives, *Meas. J. Int. Meas. Confed.* 41 (2006), pp. 121-129.
DOI: [10.1016/j.measurement.2006.03.004](https://doi.org/10.1016/j.measurement.2006.03.004)
- [17] G. M. D'Aucelli, N. Giaquinto, C. Guarnieri Caló Carducci, M. Spadavecchia, A. Trotta, Uncertainty evaluation of the Unified Method for thermo-electric module characterization, *Meas. J. Int. Meas. Confed.* 131 (2018), pp. 751-763.
DOI: [10.1016/j.measurement.2018.08.070](https://doi.org/10.1016/j.measurement.2018.08.070)
- [18] M. Yang, Z. Guan, J. Liu, W. Li, X. Liu, X. Ma, J. Zhang, Research of the instrument and scheme on measuring the interaction among electric energy Metrology of multi-user electric energy meters, *Meas. Sensors*. 18 (2021), 100067.
DOI: [10.1016/j.measen.2021.100067](https://doi.org/10.1016/j.measen.2021.100067)
- [19] E. Pittella, E. Piuze, E. Rizzuto, S. Pisa, Z. Del Prete, Metrological characterization of a combined bio-impedance plethysmograph and spectrometer, *Meas. J. Int. Meas. Confed.* 120 (2018), pp. 221-229.
DOI: [10.1016/j.measurement.2018.02.032](https://doi.org/10.1016/j.measurement.2018.02.032)
- [20] A. Ferrero, C. Muscas, On the selection of the "best" test waveform for calibrating electrical instruments under nonsinusoidal conditions, *IEEE Trans. Instrum. Meas.* 49 (2000), pp. 382-387.
DOI: [10.1109/19.843082](https://doi.org/10.1109/19.843082)
- [21] B. Qi, X. Zhao, C. Li, Methods to reduce errors for DC electric field measurement in oil-pressboard insulation based on Kerr-effect, *IEEE Trans. Dielectr. Electr. Insul.* 23 (2016), pp. 1675-1682.
DOI: [10.1109/TDEI.2016.005507](https://doi.org/10.1109/TDEI.2016.005507)
- [22] S. Corbellini, A. Vallan, Arduino-based portable system for bioelectrical impedance measurement, *IEEE MeMeA 2014 Int. Symp. Med. Meas. Appl. Proc.* (2014), pp. 4-8.
DOI: [10.1109/MeMeA.2014.6860044](https://doi.org/10.1109/MeMeA.2014.6860044)
- [23] T. Kowalski, G. P. Gibiino, J. Szewiński, P. Barmuta, P. Bartoszek, P. A. Traverso, Design, characterisation, and digital linearisation of an ADC analogue front-end for gamma spectroscopy measurements, *Acta IMEKO 10* (2021) 2, pp. 70-79.
DOI: [10.21014/acta_imeko.v10i2.1042](https://doi.org/10.21014/acta_imeko.v10i2.1042)
- [24] A. Ferrero, M. Lazzaroni, S. Salicone, A calibration procedure for a digital instrument for electric power quality measurement, *IEEE Trans. Instrum. Meas.* 51 (2002), pp. 716-722.
DOI: [10.1109/TIM.2002.803293](https://doi.org/10.1109/TIM.2002.803293)
- [25] M. Peixoto, M. V. Moreno, N. Khider, Conception of a phantom in agar-agar gel with the same bio-impedance properties as human quadriceps, *Sensors*. 21 (2021).
DOI: [10.3390/s21155195](https://doi.org/10.3390/s21155195)
- [26] L. Cristaldi, A. Ferrero, S. Salicone, A distributed system for electric power quality measurement, *IEEE Trans. Instrum. Meas.* 51 (2002), pp. 776-781.
DOI: [10.1109/TIM.2002.803300](https://doi.org/10.1109/TIM.2002.803300)
- [27] B. Sanchez, A.L.P. Aroul, E. Bartolome, K. Soundarapandian, R. Bragós, Propagation of measurement errors through body composition equations for body impedance analysis, *IEEE Trans. Instrum. Meas.* 63 (2014), pp. 1535-1544.
DOI: [10.1109/TIM.2013.2292272](https://doi.org/10.1109/TIM.2013.2292272)
- [28] T. Ouyornkochagorn, Influence of electrode placement error and contact impedance error to scalp voltage in electrical impedance tomography application, *IEECON 2019, 7th Int. Electr. Eng. Congr. Proc.* (2019).
DOI: [10.1109/iEECON45304.2019.8939016](https://doi.org/10.1109/iEECON45304.2019.8939016)